Electroweak multi-boson measurements from ATLAS and CMS: Run 1 legacy and Run 2 prospects

Luca Perrozzi for the CMS and ATLAS collaborations
Institute for Particle Physics (IPP), ETH Zürich,
Otto-Stern-Weg 5, CH - 8093 Zürich

The talk focuses on Electroweak multi-boson measurements performed by the ATLAS and CMS collaborations. An overview of the Run 1 results is presented together with prospects for Run 2 measurements.

1 Introduction

Measurements of the multi-boson production cross section test the Standard Model (SM) at the TeV scale [1]. They represent a source of irreducible background for Higgs studies and many searches for physics beyond the SM (BSM). Multi-boson production is also capable to probe boson self-interactions, searching for anomalous couplings. In particular, anomalous triple gauge couplings (aTGC) are probed by di-boson production and Electroweak (EW) production of single vector bosons, while anomalous quartic gauge couplings (aQGC) are probed by tri-boson production and EW diboson production.
The following report describes the most recent results from the ATLAS [2] and CMS [3] experiments.

1.1 Signatures and background sources

In multi-boson production processes, the signatures are represented by combinations of γ, W and Z particles, with a production cross sections hierarchy $\sigma(\gamma) > \sigma(W) > \sigma(Z)$. Multi-boson analyses feature high p_T, isolated charged leptons (electrons, muons) and possibly photons. Z bosons can be easily identified by means of an invariant mass window cut around Z pole. W bosons are selected by requiring large missing transverse energy ($\not{E}_T$) from the undetected neutrino (computed from jets, leptons and calorimeter information), together with a transverse mass selection cut. Photons appear as energy clusters in the electromagnetic calorimeter, with characteristics similar to jets.
Examples of the di-boson, vector boson fusion (VBF), tri-boson and vector boson scattering (VBS) production are reported in figure 1

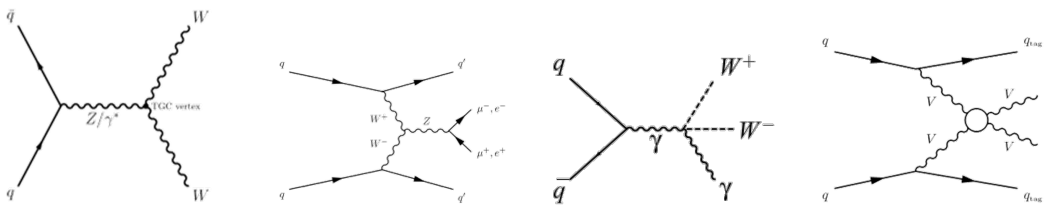

(a) Di-boson (b) VBF (c) Tri-boson (d) VBS

Figure 1 – Examples of Feynman diagrams for di-boson, VBF, tri-boson and VBS production.

1.2 Background sources

The major background sources are represented by events containing vector boson plus jets, with large cross section. In these events the high p_T leptons come from the boson or heavy flavour decays, while the jets are misidentified as charged leptons or photons. The $\not{E}_T$ is instead faked by particles falling outside acceptance. Also $t\bar{t}$ and single top events play a sizeable role, despite their lower cross section, since they naturally contain prompt isolated leptons from W bosons and large $\not{E}_T$. Finally, multi-boson processes act as background sources for each other.
The background contributions can be estimated from MC or with data-driven methods.

2 Effective theory approach to BSM

Most of the CMS and ATLAS anomalous couplings interpretations make use of the Vertex Function[4,5] approach for the neutral triple couplings ($ZZZ, Z\gamma\gamma, ZZ\gamma$) and the Effective Lagrangian[5] (though without an operator basis) for charged triple couplings ($WWW, WW\gamma$).
Only recently, a more systematic effective field theory approach (EFT) has been used to parametrize the quartic gauge anomalous couplings ($W^{\pm}W^{\pm}$ EW, $WW\gamma$, $\gamma\gamma \to WW$). In the EFT approach[6], assuming that the new physics scale Λ is separated from the EW scale v ($\Lambda \gg v$), and that the linearly realized $SU(3) \times SU(2) \times U(1)$ local symmetry is spontaneously broken by the vacuum expectation value of the Higgs doublet field, the Lagrangian of the SM can be expanded in operator dimension D:

$$\mathcal{L}_{EFT} = \mathcal{L}_{SM} + \frac{1}{\Lambda}\mathcal{L}^{D=5} + \frac{1}{\Lambda^2}\mathcal{L}^{D=6} + \frac{1}{\Lambda^3}\mathcal{L}^{D=7} + \frac{1}{\Lambda^4}\mathcal{L}^{D=8} + \dots \tag{1}$$

where the terms with $D = 5$ and $D = 7$ can be neglected at the LHC since they are lepton flavor violating, and $D = 8$ is subleading to $D = 6$. For $\mathcal{L}^{D=6}$ several complete non-redundant set of operators, each leading to a completely equivalent physics description, have been proposed in literature and are being used in the context of Higgs physics[7]. Uniformity of approach in the next generation of analyses need to be pursued in order to combine the different result and reach more stringent limits on the BSM parameters.

3 W^+W^- production and aTGC at 8 TeV in CMS

Previous ATLAS[8] and CMS[9] measurements report an excess of the W^+W^- cross section with respect to the next-to-leading order (NLO) SM prediction. A new CMS measurement[10] in the electron and muon channels has been performed, on 19.4 fb^{-1} at 8 TeV. It requires two isolated, opposite sign leptons with $p_T > 20$ GeV and pseudorapidity $|\eta_e| < 2.5$ and $|\eta_\mu| < 2.4$. The projected $\not{E}_T$ is required to be greater than 20 GeV and $p_{T,ll} > 45$ GeV. Several techniques are used to reduce the large background, including an anti b-tagging and jet veto ($N_{jets} < 2$) for $t\bar{t}$, the dilepton boost and Z mass veto for $Z + jet$ events, and a third lepton veto for WZ and ZZ. Multiple control regions are used to estimate the background yields in the signal region.
The systematic uncertainties sum up to 7.9% and are dominated by the jet veto and lepton

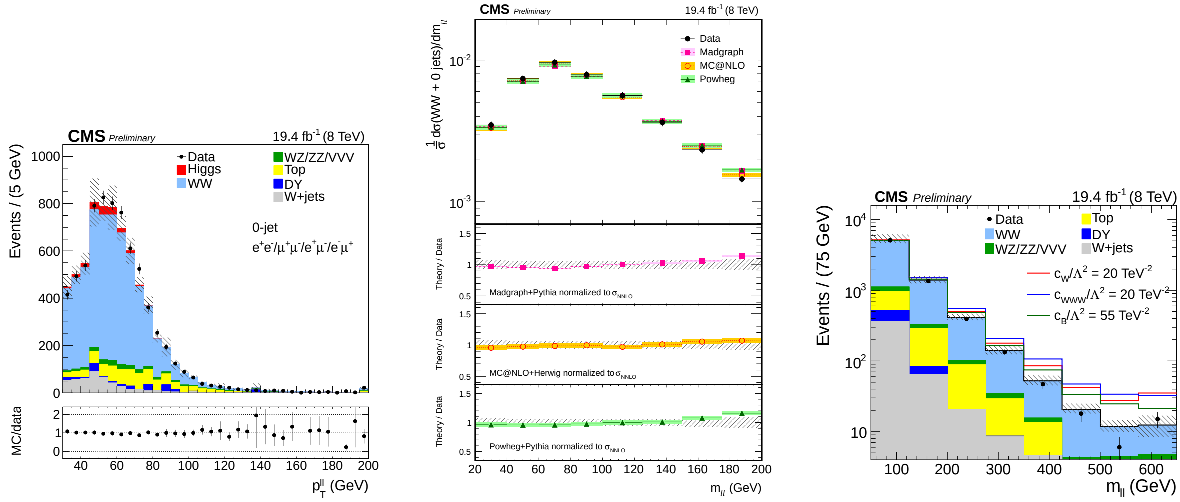

Figure 2 – Left: data and MC distributions for the 0−jet category of the p_T of the dilepton system. Center: normalized differential WW cross section as a function of the invariant mass m_{ll}. Right: m_{ll} distribution after full selection with all SM background sources compared to a given choice of the aTGC parameters.

efficiency uncertainties. The total measured cross section, after removing the Higgs contribution, is:

$$\sigma_{W^+W^-} = 60.1 \pm 0.9(\mathrm{stat}) \pm 3.2(\mathrm{exp}) \pm 3.1(\mathrm{th}) \pm 1.6(\mathrm{lumi})\ \mathrm{pb} \tag{2}$$

which is in agreement with the NNLO SM theory [11] prediction $\sigma^{NNLO}_{W^+W^-} = 59.8^{+1.3}_{1.1}$ pb.
The W^+W^- unfolded normalized differential cross section is measured as a function of kinematic variables $(p_{T,l}, m_{ll}, p_{T,ll}, \Delta\phi_{ll})$. They are compared to matrix element predictions interfaced to parton shower, and some discrepancies are observed, showing the need for improved accuracy in the calculations. Figure 2 shows the data and MC distributions for the 0−jet category of the p_T of the dilepton system, together with the normalized differential WW cross section as a function of the invariant mass m_{ll}. The latter is compared to predictions from Madgraph, Powheg and MC@NLO.
aTGC are measured in the framework of EFT operators with $D = 6$. No deviations are observed, and limits are set. Figure 2 shows the m_{ll} distribution after full selection with all SM background sources and $c_W/\Lambda^2 = 20$/TeV, $c_{WWW}/\Lambda^2 = 20$/TeV and $c_B/\Lambda^2 = 55$/TeV.

4 Evidence of $W\gamma\gamma$ production in ATLAS

The production cross section for the $W\gamma\gamma$ process [12] is measured by ATLAS in the muon and electron channels, with 20.3 fb^{-1} at 8 TeV. The analysis is performed in the fiducial phase space for the jet inclusive ($N_{jets} \geq 0$) and exclusive ($N_{jets} = 0$) cases. The systematic uncertainties are dominated by the data-driven background estimate and jet energy scale. In particular, the data-driven fake photon background from $W\gamma j$ and Wjj events is estimated with a 2D template fit to the isolation distributions of the two γ candidates.
The measured cross sections in the inclusive and exclusive case are:

$$\begin{aligned}\sigma^{N_{jets}\geq 0}_{W\gamma\gamma} &= 6.1^{+1.1}_{-1.0}(\mathrm{stat}) \pm 1.2(\mathrm{syst}) \pm 0.2(\mathrm{lumi}) \\ \sigma^{N_{jets}=0}_{W\gamma\gamma} &= 2.9^{+0.8}_{-0.7}(\mathrm{stat})^{+1.0}_{-0.9}(\mathrm{syst}) \pm 0.1(\mathrm{lumi})\end{aligned} \tag{3}$$

The significance is larger than 3σ in the inclusive case, thus representing the first evidence of $W\gamma\gamma$ production. The diphoton invariant mass distribution in the electron and muon channels is shown in figure 3. The fiducial region is defined at particle level, including jet and isolation variables. The fiducial cross section is 1.9 σ higher than the MCFM prediction in the inclusive

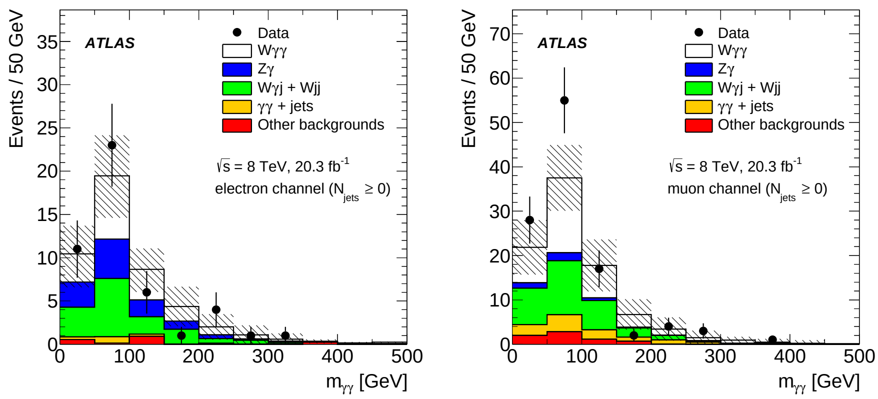

Figure 3 – Diphoton invariant mass distribution in the electron (left) and muon (right) channels. The expected signal based on the SHERPA prediction is shown. The hashed areas show the total systematic and statistical uncertainty on the background sources estimate.

case.

aQGC are measured in the framework of EFT operators with $D = 8$. Possible deviations from the SM predictions are expected in the high di-photon invariant mass. A search region is therefore defined with $m_{\gamma\gamma} > 300$ GeV. No deviations are observed, and limits are set, improving previous results published by CMS [?].

5 Updates of preliminary results

5.1 $Z\gamma$ production and aTGC at 8 TeV in CMS

CMS published [13] the measurement of the $Z\gamma$ production cross section in electron and muon channels, with 19.5 fb^{-1} at 8 TeV, whose total inclusive cross section is in agreement with theory predictions. The search for aTGC in the high $E_{T,\gamma}$ spectrum leads to limits on $ZZ\gamma$ and $Z\gamma\gamma$, improving by factor 3 the 7 TeV results.

5.2 Electroweak production of Z+2jets at 7 TeV in CMS

CMS published [15] a measurement of the EW production of Z+2jets at 7 TeV. The analysis uses a quark/gluon discriminator to reduce background, and a BDT to extract signal contribution. The measured cross section is $\sigma = 174 \pm 15(\text{stat}) \pm 40(\text{syst})$ fb and the ratio with the SM prediction is $\sigma/\sigma_{SM} = 0.84 \pm 0.07(\text{stat}) \pm 0.19(\text{syst})$. The analysis precision is limited by the knowledge of large interference effects between production diagrams. A study of the hadronic and jet activity in Z+jet events is included.

5.3 $W^{\pm}W^{\pm}$ VBS production at 8 TeV in ATLAS

ATLAS published [16] the evidence of VBS scattering in $W^{\pm}W^{\pm}$ channel at 8 TeV. The analysis is similar to the search for the Higgs decay in the WW case with VBF topology. It requires two isolated leptons with same charge, featuring a third lepton veto to reduce the WZ background contribution. It also requires two forward jets with high invariant mass and large pseudo-rapidity separation. A cut on the dilepton invariant mass $m_{ll} > 50$ GeV together with $\not{E}_T > 40$ GeV is used to reduce the W+jets and top background sources. The main residual backgrounds arise from $WZ \to 3l\nu$ and non-prompt leptons. The systematic uncertainties are dominated by jet reconstruction and theory uncertainties. In the inclusive region, the measured cross section is $\sigma = 2.1 \pm 0.5(\text{stat}) \pm 0.3(\text{syst})$ fb, corresponding to an observed significance of 4.5σ (when 3.4σ were expected). The measured cross section in the VBS enriched region, requiring $m_{jj} > 500$

GeV, is instead $\sigma = 1.3 \pm 0.4(\text{stat}) \pm 0.2(\text{syst})$ fb, corresponding to 3.6σ observed significance (when 2.8σ were expected).

6 Summary plots

The summary plots for the measured multi-boson cross sections and their ratio with theory predictions are reported in figure 4 for both ATLAS and CMS.

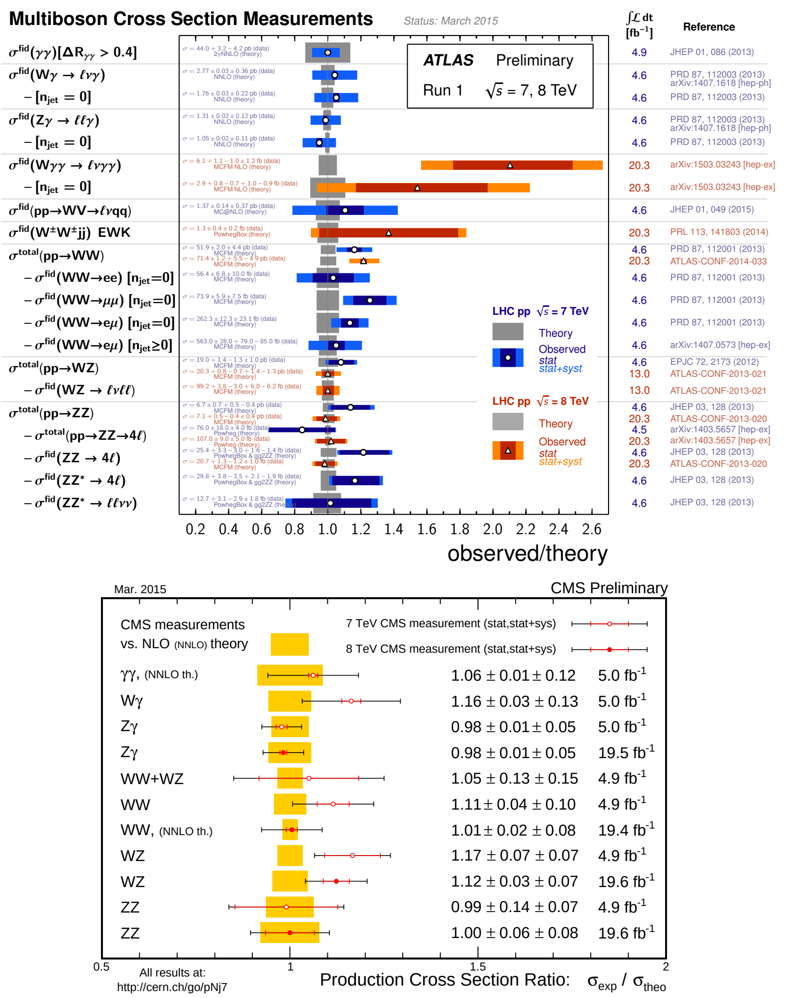

Figure 4 – Summary plots for the measured multi-boson cross sections and their ratio with theory predictions for ATLAS (top) and ratio between measured multi-boson cross sections and theory predictions for CMS (bottom).

7 Considerations towards Run 2, and long term projections

A general consideration about the precision of multi-boson measurements in Run 1 of LHC is that they are statistically limited, either in control regions or in signal regions (like high p_T or high mass). Therefore, major improvements are expected during LHC Run 2 at 13 TeV, both due to a large increases of signal cross section and much larger integrated luminosity.
However, further inputs are needed for the next round of analyses. For example, higher order MC calculations are needed to reduce the QCD scale uncertainty on the boson p_T. The NLO EW corrections are not available in most of the channels, while their contributions becomes sizeable in the search regions, i.e. high p_T or mass. Finally, very limited number of NLO MC tools is available to generate anomalous couplings.

Generally speaking about the anomalous couplings, an unitary approach is needed with other branches, like the measurements performed to characterize the Higgs sector, probing the same physics. This quest for unitary approach is needed both to combine different measurements and take into account correlated effect of BSM physics. A possible answer seems to be provided by the EFT approach, which might become the new standard, superseeding the Vertex Function and Effective Lagrangian proposed during LEP times.
From the experimental point of view, a major effort must be put in providing unfolded spectra. In particular, an important caveat is represented by the definition of the background subtracted "signal", since BSM would coherently affect different signal (and background) channels.

Long term projections on aQGC have been released in 2013 by ATLAS [17] for the VBS $WZ \to 3l\nu$, VBS $ZZ \to 4l$, VBS $W^{\pm}W^{\pm} \to 2l2\nu$, $Z \to 2l2\gamma$, and by CMS [18] for the VBS $WZ \to 3l\nu$. Depending on the new tools available and future analysis developments, however, the performance could be greatly improved.

References

1. K.A. Olive *et al.*, (Particle Data Group), Chin. Phys. C, 38, 090001 u(2014).
2. ATLAS Collaboration, "The ATLAS experiment at the CERN LHC", JINST 3 (2008) S08003.
3. CMS Collaboration, "The CMS experiment at the CERN LHC", JINST 3 (2008) S08004.
4. K. Gaemers and G.Gounaris, *Z. Phys.* C **1**, 259 (1979).
5. K. Hagiwara, *et al.*, *Nucl. Phys.* B **282**, 253 (1987).
6. C. Degrande *et al.*, "Effective Field Theory: A Modern Approach to Anomalous Couplings", (2012). arXiv:1205.4231.
7. R. Gupta *et al.*, "BSM Primary Effects", arXiv:1405.0181.
8. ATLAS collaboration, "Measurement of the W^+W^- production cross section in proton-proton collisions at $\sqrt{s} = 8$ TeV with the ATLAS detector", ATLAS-CONF-2014-033 (2014).
9. CMS collaboration, "Measurement of W^+W^- and ZZ production cross sections in pp collisions at $\sqrt{s} = 8$ TeV", *Phys. Lett.* B **721**, 190 (2013).
10. CMS collaboration, "W^+W^- cross section and anomalous gauge couplings at 8 TeV", CMS-PAS-SMP-14-016.
11. T. Gehrmann *et al.*, "W^+W^- production at hadron colliders in NNLO QCD", *Phys. Rev. Lett.* **113**, 212001 (2014).
12. ATLAS collaboration, "Evidence of $W\gamma\gamma$ production in pp collisions at $\sqrt{s} = 8$ TeV and limits on anomalous quartic gauge couplings with the ATLAS detector", (2015). arXiv:1503.03243, submitted to PRL.
13. CMS collaboration, "Measurement of the $Z\gamma$ production cross section in pp collisions at 8 TeV and search for anomalous triple gauge boson couplings", JHEP **04**, 164 (2015).
14. CMS collaboration, "A search for WW gamma and WZ gamma production and constraints on anomalous quartic gauge couplings in pp collisions at sqrt(s) = 8 TeV", PRD **90**, 032008 (2014).
15. CMS collaboration, "Measurement of EWK production of two jets in association with a Z boson in pp collisions at $\sqrt{s} = 8$ TeV", EPJC **75**, 66 (2015).
16. ATLAS collaboration, "", *Phys. Rev. Lett.* **113**, 141803 (2014).
17. ATLAS collaboration, "Studies of VBS And Triboson Production with an Upgraded ATLAS Detector at a High-Luminosity LHC", ATL-PHYS-PUB-2013-006 (2013).
18. CMS collaboration, "VBS and aQGC Studies in WZ Production at 14 TeV", CMS-PAS-FTR-13-006 (2013).